J Breast Cancer. 2019 Jun;22(2):274-284
https://doi.org/10.4048/jbc.2019.22.e28
pISSN 1738-6756·eISSN 2092-9900

Journal of Breast Cancer JBC

Original Article

Murine Model Study of a New Receptor-Targeted Tracer for Sentinel Lymph Node in Breast Cancer

Chonglin Tian [1,2], **Xiao Sun** [2], **Binbin Cong** [1,2], **Pengfei Qiu** [2], **Yongsheng Wang** [2]

[1]School of Medicine and Life Sciences, University of Jinan and Shandong Academy of Medical Sciences, Jinan, China
[2]Breast Cancer Center, Shandong Cancer Hospital affiliated to Shandong University, Shandong Academy of Medical Sciences, Jinan, China

Received: Jan 27, 2019
Accepted: May 13, 2019

Correspondence to
Yongsheng Wang
Breast Cancer Center, Shandong Cancer Hospital affiliated to Shandong University, 440 Jiyan Rd, Jinan 250117, China.
E-mail: wangysh2008@aliyun.com

ORCID iDs
Chonglin Tian
https://orcid.org/0000-0002-4186-2024
Xiao Sun
https://orcid.org/0000-0002-3475-6602
Binbin Cong
https://orcid.org/0000-0002-8026-2988
Pengfei Qiu
https://orcid.org/0000-0001-8644-1445
Yongsheng Wang
https://orcid.org/0000-0001-6252-684X

Conflict of Interest
The authors declare that they have no competing interests.

ABSTRACT

Purpose: Sentinel lymph node biopsy (SLNB), a critical staging and treatment step, has replaced axillary lymph node (LN) dissection as the standard staging procedure for early stage breast cancer patients with clinically negative axillary LNs. Hence, using a murine sentinel lymph node (SLN) model, we investigated the localization effect of the new receptor-targeted tracer, indocyanine green (ICG)-rituximab, on breast cancer SLNB.
Methods: After establishing the murine SLN model, different doses of ICG-rituximab were subcutaneously injected into the hind insteps of BALB/c mice to determine the optimal dose and imaging time using continuous (> 3 hours) MDM-I fluorescence vasculature imaging. To explore the capacity of ICG-rituximab for sustained SLN localization with the optimal dose, MDM-I imaging was monitored at 6, 12, and 24 hours.
Results: The popliteal LN was defined as the SLN for hindlimb lymphatic drainage, the iliac LN as the secondary, and the para-aortic or renal LN as the tertiary LNs. The SLN initial imaging and optimal imaging times were shortened with increased ICG-rituximab doses, and the imaging rates of the secondary and tertiary LNs increased accordingly. The optimal ICG dose was 0.12 μg, and its optimal imaging time was 34 minutes. After 24 hours, the SLN imaging rate remained 100%, while those of the secondary and the tertiary LNs increased from 0% (6 hours) and 0% (6 hours) to 10% (12 hours) and 10% (12 hours) to 20% (24 hours) and 10% (24 hours), respectively.
Conclusion: ICG-rituximab localized to the SLN without imaging from the secondary or tertiary LNs within 6 hours. The optimal ICG dose was 0.12 μg, and the optimal interval for SLN detection was 34 minutes to 6 hours post-injection. This novel receptor-targeted tracer is of great value to clinical research and application.

Keywords: Animal model; Indocyanine green; Rituximab; Sentinel lymph node; Synthetic imaging agent

Author Contributions

Data curation: Tian C, Cong B; Formal analysis: Tian C; Funding acquisition: Wang Y; Methodology: Tian C, Sun X, Wang Y; Project administration: Tian C, Sun X, Wang Y; Resources: Tian C, Cong B; Software: Qiu P; Writing - original draft: Tian C; Writing - review & editing: Wang Y.

INTRODUCTION

Sentinel lymph node biopsy (SLNB) has replaced axillary lymph node (LN) dissection as the standard staging procedure for early stage breast cancer patients with clinically negative axillary LNs [1-4]. Globally, clinical guidelines recommend a combination of technetium-labelled sulfur colloid and blue dye as SLNB tracers. However, the extensive use of radionuclides is limited because of the associated radiation exposure, mandatory licensing requirements, and restricted availability [5-7]. Therefore, many institutions still employ a single-dye method when performing SLNB, often leading to unsatisfactory success rates and relatively high false-negatives, even when conducted by experienced surgeons. This presents the need for an improved or new SLNB procedure involving the use of very limited or no radioisotopes.

An 'ideal' contrast agent would be one that imposes little risk to patient health, is highly specific to sentinel lymph node (SLN), optimizes lymphatic uptake and migration speed, creates a high signal to noise ratio (e.g. good retention and distinguishable from background signals), can be detected with high resolution and in low quantities (sensitivity), and is relatively easy and economical to use. Indocyanine green (ICG), which is affordable and has low toxicity, yields a fluorescent signal that has been used to locate SLNs in breast cancer with a reliably high signal-to-background ratio (SBR) [8]. However, tracking SLNs by following fluorescently labeled lymphatic vessels usually results in several false-negatives, owing to insufficient dye penetration (< 1 cm) and thin lymphatic vessels [9], as deep lymphatic vessels and LNs cannot be clearly observed. Rituximab is a specific humanized monoclonal antibody that targets CD20 molecules on the surfaces of B cells in LNs [10]. Considering the positive attributes of ICG and rituximab, we hypothesized that a combination of both makes an ideal new tracer to facilitate SLNB for breast cancer treatment. Furthermore, a successful combination will have dual advantage of a fluorescent tracer and a lymphatic-targeted drug, resulting in significant clinical applications.

In this study, we used hindlimb drainage in mice to mimic tracer-based SLNB in breast cancer patients. Using this model, we determined several parameters for mapping murine SLNs, including the optimal injection dose, imaging time, and imaging rate for secondary LNs. These results should lay the foundation for potential future clinical research and applications in breast cancer SLNB, as well as other cancers.

METHODS

Main experimental materials

Materials included rituximab (100 mg) (F. Hoffmann-La Roche, Ltd, Basel, Switzerland); indocyanine green (25 mg) (Dandong Yichuang Pharmaceutical, Ltd, Liaoning, China); semi-permeable membranes with a diameter of 22 mm and a molecular weight cut-off of 4,000–6,000 Da (Spectrum Laboratories, Inc., Rancho Dominguez, USA); the neoprobe 2000 handheld γ detector (Johnson & Johnson, New Brunswick, USA); cyclone phosphor screen imaging system (Packard Company, California City, USA); the MDM-I fluorescence vasculature imaging system (Mingde Biotech, Ltd, Langfang, China); and sterile, female BALB/c mice weighing 18–22 g (HFK Bioscience, Beijing, China).

Establishing the murine SLN model

Initially, a literature search was done to identify the anatomical nomenclature used for murine LNs [11] to increase efficiency and accuracy when applying combined tracing of SLNs in 10

https://doi.org/10.4048/jbc.2019.22.e28

Journal of Breast Cancer JBC

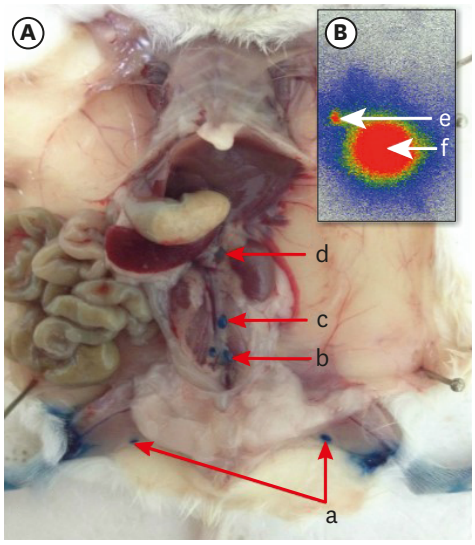

Figure 1. Lymphatic drainage system in the mouse hindlimb. (A) popliteal lymph node (a); iliac lymph node (b); lumbar aortic lymph nodes (c); and renal lymph node (d). (B) Each mouse was placed under a Cyclone phosphor screen imager to record an image popliteal lymph node (e); injection point (f).

BALB/c mice. Specifically, 10 μL of technetium 99m (^{99m}Tc)-labelled sulfur colloid (5 μCi) was injected subcutaneously into the hind instep of each mouse. Three hours later, each mouse was placed under a Cyclone phosphor screen imager for image recording (**Figure 1B**). Each mouse was then sacrificed via cervical dislocation and subjected to popliteal dissection to drain their LNs. Five minutes prior to the dissection, methylene blue was administered as described above. The stained popliteal, iliac, para-aortic, and renal LNs were collected using a handheld γ detector, and we then measured the average radionuclide count for each of these nodes. Based on the radionuclide detection results, the threshold value of SLN was defined as 10% of the highest count. All animal experiments were approved by Shandong Cancer Hospital affiliated to Shandong University Animal Ethics Committee (Approval number, No. SDTHEC201603008), and animal use complied with the international principles of animal use.

Preparing the receptor-targeted tracer

Our previous studies revealed that the optimal coupling mass ratio between ICG and rituximab is 1:4, and the resulting conjugate, which is a sterile non-local-injection injury tracer with no acute toxicity, retained the molecular integrity and immune function of rituximab. The coupling procedure was performed as follows:

Firstly, at room temperature and in the dark, 100 mg of rituximab was mixed with 10 mL of sterile water to yield a 10 mg/mL solution, and 25 mg of ICG was mixed with 10 mL of sterile water to generate a 2.5 mg/mL solution.

Secondly, the ICG solution was mixed in a dropwise manner with the rituximab solution at the optimal coupling ratio, and the reaction mixture was immediately homogenized for 5 minutes using a magnetic stirrer. The mixture was centrifuged at 3,000 rpm for 20 minutes, and the resulting supernatant was placed into a dialysis bag prepared with a semi-permeable membrane.

Thirdly, the coupling mixture in the dialysis bag was submerged in 200 of previously sterilized injection water and dialyzed, and the sterile water was changed every 2 hours. The ICG-rituximab conjugation product was then collected.

https://doi.org/10.4048/jbc.2019.22.e28

The receptor-targeted tracer label rate was analyzed using instant thin-layer chromatography-silica gel. In the reaction system 1, the volume ratio of pyridine:ethanol:water was 5:2:1. The reaction system 2 was acetone. To observe for the critical point of the reaction when using the reaction system 1, ICG was expected to be at base point and the receptor-targeted tracer at the front of the test strip. When using the reaction system 2, rituximab and the receptor-targeted tracer were expected to be at base point and ICG at the front of the test strip.

Bacteria detection

The new tracer was incubated in cell culture mediums at 37°C for 1 week to ensure the absence of bacteria contaminants.

Pyrogen detection

The bacterial endotoxin of the new tracer was detected using Limulus tests. *Escherichia coli* endotoxin was used as positive control, and sterile injection water was used as negative control. If the reaction solution was jelly-like, then pyrogen was present in the new tracer. If the reaction solution was clear, then the new tracer was pyrogen free.

Toxicity test

Six-week-old female BALB/c mice were divided into 5 groups with 4 mice per group. Five different mass ratios of ICG-rituximab were intradermally injected into the mouse hind paw at doses of 1.2 mg/kg and 12 mg/kg (10 and 100 times that of humans). After injection, the mice were fed under specific pathogen-free conditions in a basic laboratory at Shandong Cancer Hospital affiliated to Shandong University and observed for 2 weeks.

Experimental procedures

The experiment was conducted in 2 steps. The murine SLN model (results section) was first used to determine the optimal injection dose and imaging time of ICG-rituximab, using a dose-escalation test. Secondly, after injecting the optimal doses of ICG-rituximab and ICG (all subgroups of 10 mice each), the imaging rates of secondary LNs were compared to investigate the localization ability of ICG-rituximab.

Determining the optimal injection dose and imaging time

Experimental group

Ten microliters of ICG-rituximab (containing either: 0.48 μg, 0.24 μg, 0.12 μg, or 0.06 μg of ICG) was subcutaneously injected into the hind instep of each mouse of each subgroup. After the injections, the MDM-I fluorescence vascular imager was used to continuously monitor the SLN in each mouse and produce images at 5-minute intervals over 3 hours. The initiation and optimal imaging times required to observe SLN fluorescence were recorded. The mice were sacrificed via cervical dislocation after 3 hours, prior to the dissection of the popliteal space and lymph node drainage. Five minutes prior to the dissections, methylene blue was injected into the mice using the same procedure described above. The stained SLNs, secondary LNs, and tertiary LNs were collected, and the MDM-I fluorescence vascular imager was then used to detect the presence or absence of fluorescent signals.

Control group

A total of 0.12 μg of ICG in a 10-μL volume was subcutaneously injected into the hind instep of each mouse. The MDM-I fluorescence vascular imager was used to continuously monitor the popliteal SLN until a visible signal was attained, after which point images were captured every 5 minutes for 3 hours. The initiation and optimal imaging times required to observe

https://doi.org/10.4048/jbc.2019.22.e28

SLN fluorescence were recorded. The subsequent steps are the same as described in the paragraph above.

Observation of continual SLN mapping

Experimental group

The ICG-rituximab solution (10 μL, containing 0.12 μg of ICG) was subcutaneously injected into the hind instep of each mouse. The mice were divided into 3 subgroups, and sacrificed via cervical dislocation at 6-, 12-, or 24-hour post-injection. Subsequently, the popliteal space was dissected. Five minutes prior to dissection, methylene blue was injected into the mice as described above. The stained SLNs, secondary LNs, and tertiary LNs were collected, and the MDM-I fluorescence vascular imager was then used to detect the presence or absence of fluorescence.

Control group

The ICG solution (10 μL, containing 0.12 μg of ICG) was subcutaneously injected into the hind instep of each mouse. The mice were divided into 3 subgroups. The subsequent procedures are the same as described in the paragraph above.

RESULTS

Establishing the murine SLN model

The radionuclide counts for the popliteal, iliac, para-aortic, and renal LNs were 35.50 ± 6.75, 2.00 ± 1.15, 0.00 ± 0.00, and 0.00 ± 0.00, respectively. We thus defined the popliteal lymph node as the SLN for hindlimb lymphatic drainage, the iliac lymph node as the secondary LN, and the para-aortic or renal LN (in mice where the para-aortic LN was absent) as the tertiary LNs. Concurrently, the SLN location targeted by the radionuclide was verified as consistent with the primary node, traced using lymphatic drainage to observe the injected dye (**Figure 1**).

Preparing the receptor-targeted tracer

In reaction system 1, the receptor-targeted tracer was found at the front of the test strip. In reaction system 2, rituximab and the receptor-targeted tracer were identified at base point. The ICG label rate of rituximab was 100%.

Safety limitation test

No bacteria contaminants were identified in the new tracer solution. The limulus tests resulted in a clear reaction solution, indicating that the new tracer was pyrogen free. The acute and local toxicity tests showed no mice deaths and no skin or allergic reaction, respectively.

Determining the optimal injection dose and imaging time

Increasing the ICG-rituximab injection dose from 0.06 μg to 0.48 μg decreased the SLN fluorescence initiation and the optimal imaging times from 18.4 minutes and 39.6 minutes to 8.0 minutes and 21.9 minutes, respectively. In addition, increasing the tracer dose from 0.06 μg to 0.48 μg led to a corresponding gradual increase in the imaging rate of the secondary LN from 0% to 90%, and of the tertiary LN from 0% to 90%. In contrast, the group treated solely with ICG tracer yielded imaging rates of 100% and 90% for the secondary and tertiary LNs at 3 hours, respectively (**Table 1**). The secondary and tertiary LNs were easily identifiable at the 0.24 μg ICG dose, as opposed to the 0.06 μg dose, where the SLN images were relatively low

https://doi.org/10.4048/jbc.2019.22.e28

Table 1. Lymph node imaging at all levels after the administration of different doses of ICG-rituximab

Dose (μg)	SLN		3 hr		
	Imaging time (min)	Optimal imaging time (min)	SLN	Secondary	Tertiary
0.06	18.40 ± 2.46	39.60 ± 3.63	100% (10/10)	0% (0/10)	0% (0/10)
0.12	10.50 ± 1.72	34.30 ± 2.79	100% (10/10)	0% (0/10)	0% (0/10)
0.24	8.30 ± 2.21	29.70 ± 4.00	100% (10/10)	30% (3/10)	20% (2/10)
0.48	8.00 ± 1.70	21.90 ± 4.01	100% (10/10)	90% (9/10)	90% (9/10)
0.12*	9.10 ± 1.37	28.00 ± 3.13	100% (10/10)	100% (10/10)	90% (9/10)

ICG-Rituximab, = indocyanine green-rituximab; SLN = sentinel lymph node.
*ICG in the control group.

in fluorescence intensity. Therefore, a dose of 0.12 μg was adopted as the optimal injection dose, which yielded an optimal imaging time of 34-minute post-injection (**Figure 2**).

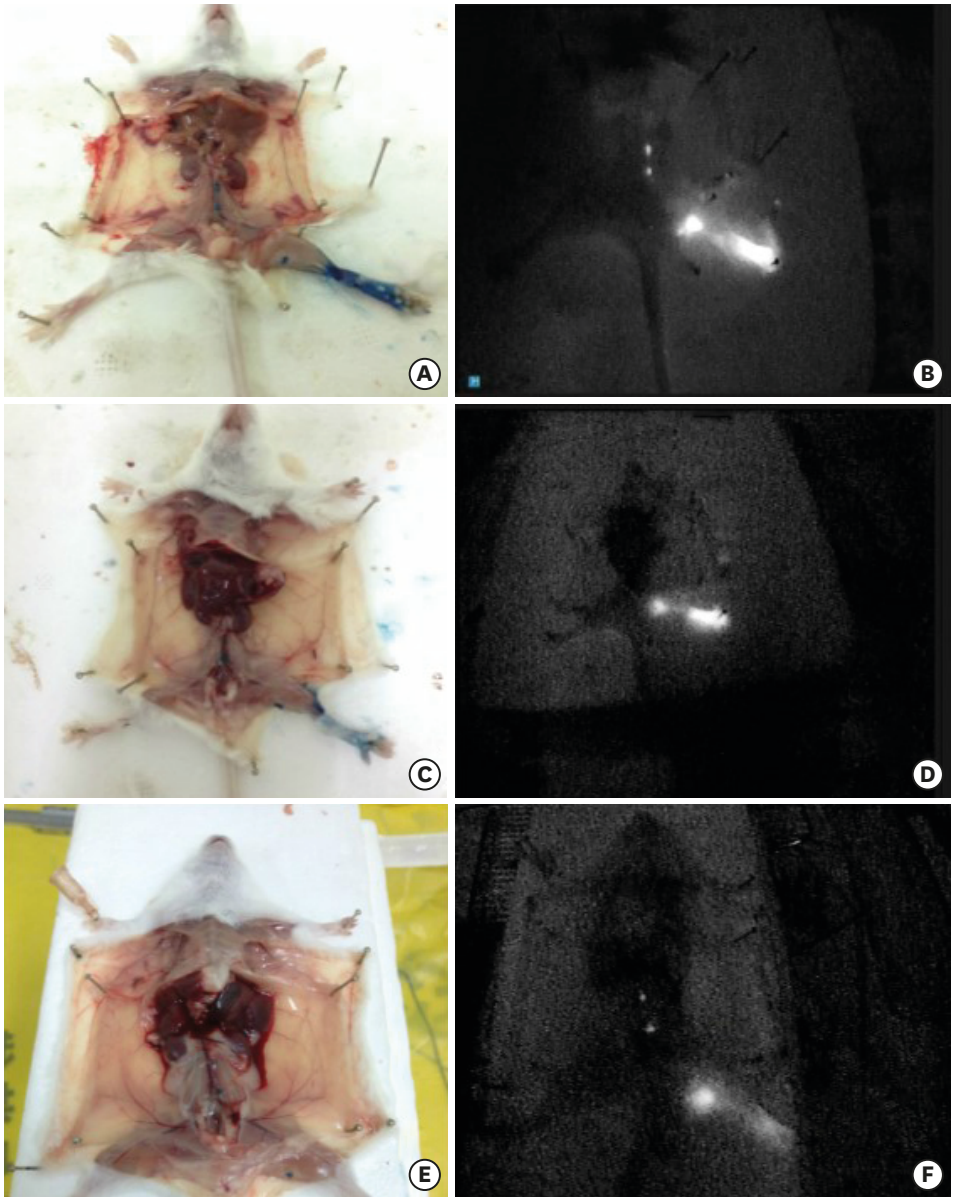

Figure 2. Comparison between a high and low dose of the new tracer. (A, B) High dose of ICG-rituximab (0.48 μg); (C, D) low dose of ICG-rituximab (0.12 μg); and (E, F) ICG (0.12 μg).
ICG = indocyanine green.

https://doi.org/10.4048/jbc.2019.22.e28

Table 2. Lymph nodes imaging at all levels after 3 hours

Dose (μg)	6 hr			12 hr			24 hr		
	SLN	Secondary	Tertiary	SLN	Secondary	Tertiary	SLN	Secondary	Tertiary
0.12	100% (10/10)	0% (0/10)	0% (0/10)	100% (10/10)	10% (1/10)	10% (1/10)	100% (10/10)	20% (2/10)	10% (1/10)
0.12*	100% (10/10)	80% (8/10)	70% (7/10)	30% (3/10)	30% (3/10)	10% (1/10)	10% (1/10)	0% (0/10)	0% (0/10)

SLN = sentinel lymph node; ICG = indocyanine green.
*ICG in the control group.

Continual mapping of the SLN

Following the administration of the optimal dose of ICG-rituximab, the ICG-rituximab-treated group maintained a stable SLN imaging rate of 100%. In addition, the imaging rates of the secondary and tertiary LNs increased from 0% and 0% at 6 hours to 20% and 10% at 24 hours, respectively (**Table 2**, **Figures 3** and **4**). For the group solely receiving the ICG tracer, the SLN imaging rate decreased from 100% at 6 hours to 10% at 24 hours. Similarly, the

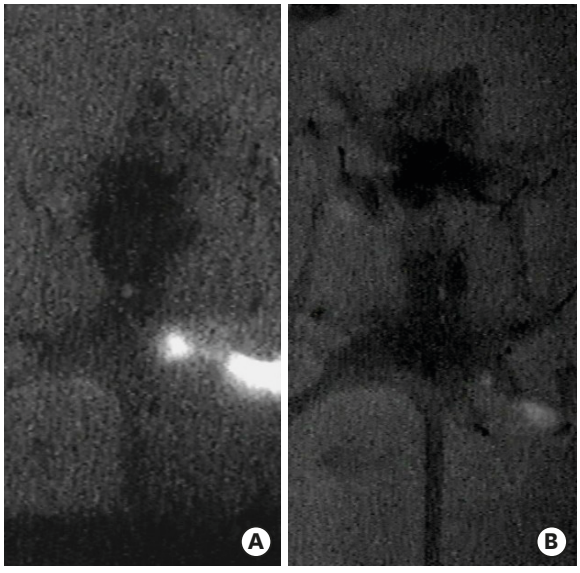

Figure 3. Lymph node imaging at secondary and tertiary LN levels after 12-hr post ICG-rituximab injection.
(A) ICG-rituximab (0.12 μg); (B) ICG (0.12 μg).
LN = lymph node; ICG = indocyanine green.

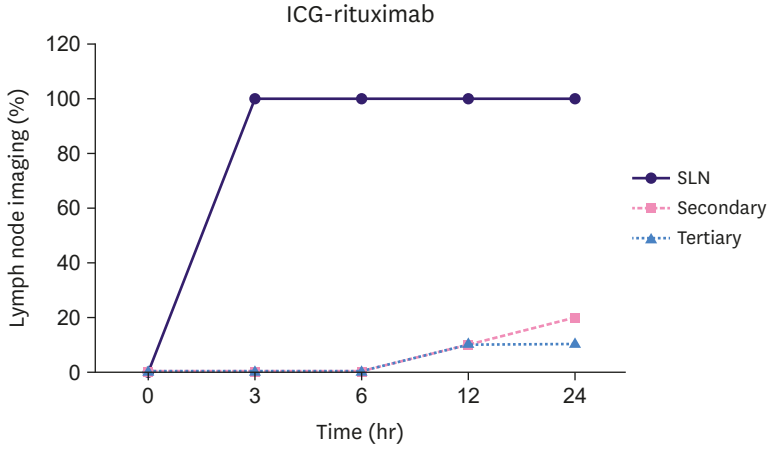

Figure 4. Continual mapping of the LNs post ICG-rituximab (0.12 μg) injection. SLN imaging rate was maintained at 100%. The imaging rates of the secondary and tertiary LNs increased with time, respectively.
SLN = sentinel lymph node, LNs = lymph nodes; ICG = indocyanine green.

https://doi.org/10.4048/jbc.2019.22.e28

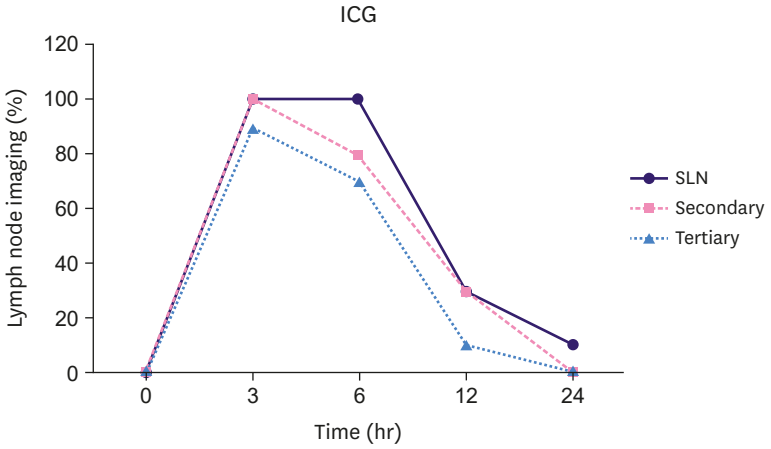

Figure 5. Continual mapping of the LNs post IGC (0.12 μg) injection. The imaging rates of LNs at all levels decreased with time.
SLN = sentinel lymph node, LNs = lymph nodes; ICG = indocyanine green.

imaging rates of the secondary and tertiary LNs decreased from 80% and 70% at 6 hours to 0% and 0% at 24 hours, respectively (**Table 2**, **Figures 3** and **5**).

DISCUSSION

As a minimally invasive biopsy technique for accurate axillary staging, SLNB represents the peak of current breast cancer surgical treatments [12-14]. It is now well established that the status of the SLN is a reliable indicator of the status of non-SLN regional nodes and is ultimately a strong independent prognostic marker for the patient. To achieve a relatively high success rate and low false-positives for SLNB, the use of a combination of technetium-labeled sulfur colloid and blue dye is recommended [15]. However, the widespread use of radiolabeled colloids is restricted due to several limitations associated with such reagents [16]. ^{99m}Tc for example has a 6-hour half-life, limiting its availability to proximal centers that handle its parent isotope molybdenum-99 (^{99}Mo). ^{99}Mo must also be supplied to nuclear medicine departments of hospitals every 2 weeks because it decays rapidly. Furthermore, it is only produced in a few reactors globally. Additionally, the supply of ^{99}Mo becomes interrupted when nuclear facilities are refurbished or compromised. Moreover, the use of radioisotopes challenges the logistics of hospitals with respect to proper handling and radioactive waste disposal, staff training, as well as meeting up with various legislative requirements, among other concerns. Additionally, surgery schedules are restricted by the 6-hour half-life of ^{99m}Tc because members of nuclear medicine departments must perform the injections of this compound as opposed to surgeons [17]. Finally, patients may object to radiation exposure.

Fluorescence imaging is at the forefront of emerging tracing technologies. ICG, a fluorescent tracer, can be excited by a near-infrared light (760 nm) source housed within a fluorescence vascular imaging system to generate fluorescent emission (820–830 nm) after injection into breast tissue. This fluorescence can penetrate human tissue, and the imager can then be used to clearly monitor lymphatic drainage and the SLN. However, due to the small particle size of ICG, this method allows the transcutaneous visualization of lymphatic vessels and intraoperative orientation during tissue dissection for SLN identification for a maximum duration of only 30 min, while simultaneously revealing high imaging rates for secondary

https://doi.org/10.4048/jbc.2019.22.e28

LNs [5,16,18]. Rituximab is a humanized monoclonal antibody that specifically targets CD20 molecules expressed on the surfaces of B cells in LNs. This protein also includes domains capable of binding to other small molecules. In this study, we tested a new tracer, ICG-rituximab, which is a conjugate of a fluorescent tracer and the lymphatic-targeting drug. The large antibody rituximab was coupled to the smaller tracer molecule ICG, and the resulting conjugate possessed the properties of both moieties. More so, the conjugate is easy to produce, is non-radioactive, and can bind to SLNs to generate a fluorescent signal upon excitation with near infrared light, allowing for specific SLN mapping. Therefore, performing SLNB with this conjugate eliminates the method of following fluorescently labeled lymphatic vessels to track SLNs. Instead, the SLN can be identified using an infrared fluorescence imaging system during surgery. As such, fluorescently labeled SLNs can be surgically isolated from surrounding tissues, avoiding non-dissected SLNs and fluorescence contamination from neighboring tissues.

Clinical practice and literature reports show that axillary LNs drain lymph fluid throughout the breast, independent of tumor and tracer injection sites. Hence, a healthy murine SLN model was used. The model used in this study is technically simple to set up; the operation is simple to perform and has the advantages of other low-cost rodent models. Based on our results, the dose of ICG-rituximab can dramatically affect image acquisition of the SLN and secondary draining LNs. Specifically, increasing the injection dose decreased the SLN fluorescence initiation and optimal imaging times, while the development rates for the secondary and tertiary LNs gradually increased. These results indicate that ICG-rituximab can reach saturation, such that when the levels of the administered conjugate surpass the binding capacity of CD20 molecules on B cells in the SLN, the excess tracer will drain into the secondary and tertiary LNs. As a consequence, the secondary and tertiary LNs will fluoresce. However, when ICG-rituximab was administered at a dose of 0.12 μg, the secondary and tertiary LNs did not produce images until 12-hour post-injection. Furthermore, from 0- to 24-hour post-injection, the SLN imaging rate was sustained at 100%, while the fluorescence in the secondary and tertiary LNs was below 20%. When the same dose of solely ICG was used, the secondary and tertiary LNs displayed imaging rates of 100% and 90%, respectively, at 3-hour post-administration, with a gradual reduction in all (SLN and next-level LNs) imaging rates over the course of 24-hour post-injection. These results suggest that when ICG enters draining LNs, a large proportion of the molecule is metabolized by the liver because it cannot anchor to CD20 molecules present in the LNs without being coupled to rituximab. As a consequence, the imaging rates of the SLN and the secondary and tertiary LNs gradually decrease over time.

The main limitation of this study is the insufficient fluorescence penetration, which makes it challenging to identify SLNs during surgery. In addition, after a long time, the residual ICG-rituximab at the injection site continually drains slowly into the SLN, and the level of the administered conjugate finally surpasses the binding capacity of the CD20 molecules on the SLN B cells. As a result, 12-hour post ICG-rituximab injection, the secondary and tertiary LNs of the treated mice started generating a signal, although imaging rates were at basal level and the fluorescence intensities of the secondary LNs were much lower than that of the SLN (**Figure 3A**). The conjugate did not prevent neighboring LNs from fluorescing (**Table 2**). Therefore, related research is ongoing to examine the fluorescence intensities of SLNs translating qualitative fluorescence-negative or fluorescence-positive information into quantitative data reflective of different light intensities. In addition, the determination of threshold levels of fluorescence intensity for this conjugate tracer may be required to further

https://doi.org/10.4048/jbc.2019.22.e28

optimize ICG-rituximab use in breast cancer treatment. We believe that further studies involving this receptor-targeted tracer will promote its use in clinical research and application.

Overall, we created a new SLN tracer by conjugating ICG to rituximab (coupling mass ratio, 1:4) and used murine hindlimb lymphatic drainage as a model to determine the optimal dose of ICG-rituximab as 0.12 μg (dose of ICG) and to attain the optimal period for SLN detection (34-minute to 6-hour post-injection) without imaging noise from the secondary or tertiary LNs. Based on these results, this tracer shows great promise for clinical research and application.

REFERENCES

1. Lyman GH, Temin S, Edge SB, Newman LA, Turner RR, Weaver DL, et al. Sentinel lymph node biopsy for patients with early-stage breast cancer: American Society of Clinical Oncology clinical practice guideline update. J Clin Oncol 2014;32:1365-83.
PUBMED | CROSSREF
2. Veronesi U, Paganelli G, Galimberti V, Viale G, Zurrida S, Bedoni M, et al. Sentinel-node biopsy to avoid axillary dissection in breast cancer with clinically negative lymph-nodes. Lancet 1997;349:1864-7.
PUBMED | CROSSREF
3. Krag DN, Anderson SJ, Julian TB, Brown AM, Harlow SP, Ashikaga T, et al. Technical outcomes of sentinel-lymph-node resection and conventional axillary-lymph-node dissection in patients with clinically node-negative breast cancer: results from the NSABP B-32 randomised phase III trial. Lancet Oncol 2007;8:881-8.
PUBMED | CROSSREF
4. Zavagno G, De Salvo GL, Scalco G, Bozza F, Barutta L, Del Bianco P, et al. A randomized clinical trial on sentinel lymph node biopsy versus axillary lymph node dissection in breast cancer: results of the Sentinella/GIVOM trial. Ann Surg 2008;247:207-13.
PUBMED | CROSSREF
5. Hirche C, Murawa D, Mohr Z, Kneif S, Hünerbein M. ICG fluorescence-guided sentinel node biopsy for axillary nodal staging in breast cancer. Breast Cancer Res Treat 2010;121:373-8.
PUBMED | CROSSREF
6. Stratmann SL, McCarty TM, Kuhn JA. Radiation safety with breast sentinel node biopsy. Am J Surg 1999;178:454-7.
PUBMED | CROSSREF
7. Wishart GC, Loh SW, Jones L, Benson JR. A feasibility study (ICG-10) of indocyanine green (ICG) fluorescence mapping for sentinel lymph node detection in early breast cancer. Eur J Surg Oncol 2012;38:651-6.
PUBMED | CROSSREF
8. Chi C, Ye J, Ding H, He D, Huang W, Zhang GJ, et al. Use of indocyanine green for detecting the sentinel lymph node in breast cancer patients: from preclinical evaluation to clinical validation. PLoS One 2013;8:e83927.
PUBMED | CROSSREF
9. Vahrmeijer AL, Hutteman M, van der Vorst JR, van de Velde CJ, Frangioni JV. Image-guided cancer surgery using near-infrared fluorescence. Nat Rev Clin Oncol 2013;10:507-18.
PUBMED | CROSSREF
10. Reff ME, Carner K, Chambers KS, Chinn PC, Leonard JE, Raab R, et al. Depletion of B cells *in vivo* by a chimeric mouse human monoclonal antibody to CD20. Blood 1994;83:435-45.
PUBMED
11. Van den Broeck W, Derore A, Simoens P. Anatomy and nomenclature of murine lymph nodes: descriptive study and nomenclatory standardization in BALB/cAnNCrl mice. J Immunol Methods 2006;312:12-9.
PUBMED | CROSSREF
12. Turner RR, Ollila DW, Krasne DL, Giuliano AE. Histopathologic validation of the sentinel lymph node hypothesis for breast carcinoma. Ann Surg 1997;226:271-8.
PUBMED | CROSSREF
13. Krag D, Weaver D, Ashikaga T, Moffat F, Klimberg VS, Shriver C, et al. The sentinel node in breast cancer--a multicenter validation study. N Engl J Med 1998;339:941-6.
PUBMED | CROSSREF

14. Veronesi U, Paganelli G, Viale G, Luini A, Zurrida S, Galimberti V, et al. A randomized comparison of sentinel-node biopsy with routine axillary dissection in breast cancer. N Engl J Med 2003;349:546-53.
PUBMED | CROSSREF

15. Degnim AC, Oh K, Cimmino VM, Diehl KM, Chang AE, Newman LA, et al. Is blue dye indicated for sentinel lymph node biopsy in breast cancer patients with a positive lymphoscintigram? Ann Surg Oncol 2005;12:712-7.
PUBMED | CROSSREF

16. Ahmed M, Purushotham AD, Douek M. Novel techniques for sentinel lymph node biopsy in breast cancer: a systematic review. Lancet Oncol 2014;15:e351-62.
PUBMED | CROSSREF

17. Kelley LM, Holmes DR. Tracer agents for the detection of sentinel lymph nodes in breast cancer: current concerns and directions for the future. J Surg Oncol 2011;104:91-6.
PUBMED | CROSSREF

18. Guo W, Zhang L, Ji J, Gao W, Liu J, Tong M. Breast cancer sentinel lymph node mapping using near-infrared guided indocyanine green in comparison with blue dye. Tumour Biol 2014;35:3073-8.
PUBMED | CROSSREF